

Scaling and Evolution of Stellar Magnetic Activity

Emre Işık^{1,2†}, Jennifer L. van Saders^{3†}, Ansgar Reiners^{4*†}
and Travis S. Metcalfe^{5†}

¹Max-Planck-Institut für Sonnensystemforschung,
Justus-von-Liebig-Weg 3, Göttingen, 37077, Germany.

²Department of Computer Science, Turkish-German University,
Şahinkaya Cd. 94, Beykoz, 34820, Istanbul, Turkey.

³Institute for Astronomy, University of Hawaii, 2680 Woodlawn
Dr., Honolulu, Hawaii 96822, USA.

^{4*}Institut für Astrophysik und Geophysik,
Georg-August-Universität Göttingen, Friedrich-Hund-Platz 1,
Göttingen, 37077, Germany.

⁵White Dwarf Research Corporation, 9020 Brumm Trl, Golden,
Colorado 80403, USA.

*Corresponding author(s). E-mail(s):

Ansgar.Reiners@phys.uni-goettingen.de;

Contributing authors: isik@mps.mpg.de; jlvs@hawaii.edu;
travis@wdrc.org;

†These authors contributed equally to this work.

Abstract

Magnetic activity is a ubiquitous feature of stars with convective outer layers, with implications from stellar evolution to planetary atmospheres. Investigating the mechanisms responsible for the observed stellar activity signals from days to billions of years is important in deepening our understanding of the spatial configurations and temporal patterns of stellar dynamos, including that of the Sun. In this paper, we focus on three problems and their possible solutions. We start with direct field measurements and show how they probe the dependence of magnetic flux and its density on stellar properties and activity indicators. Next, we review the current state-of-the-art in physics-based models of photospheric

activity patterns and their variation from rotational to activity-cycle timescales. We then outline the current state of understanding in the long-term evolution of stellar dynamos, first by using chromospheric and coronal activity diagnostics, then with model-based implications on magnetic braking, which is the key mechanism by which stars spin down and become inactive as they age. We conclude by discussing possible directions to improve the modeling and analysis of stellar magnetic fields.

Keywords: Cool Stars, Stellar Magnetism, Stellar Activity, Angular Momentum Loss

1 Overview

Magnetism is ubiquitous in stars and yet it is relatively poorly understood, even in our closest neighbor. We necessarily rely on observational constraints—direct measurements or proxies for magnetism—to probe magnetic behavior across stellar types and lifetimes, and to connect these observations to underlying theoretical descriptions (Schrijver and Zwaan, 2000). In this paper, we highlight ways in which magnetism on stars reveals itself, and the insights those physical manifestations provide about the underlying physics of magnetic fields in stellar systems. The purpose of this paper is to report on recent progress in the following particular problems.

- How does magnetic flux and its density scale with rotation and the fractional depth of the convection-zone?
- How can physics-based diagnostic modeling help us to constrain surface patterns and their evolution?
- What is responsible for the spin-down and the weakening of outer-atmospheric activity indicators with age?

Following a summary of our recent attempts to find answers to these questions, we present an outlook on possible avenues to better understand the scaling relations of stellar magnetic activity. More extensive reviews can be found in the literature (e.g., Donati and Landstreet, 2009; Strassmeier, 2009; Reiners, 2012; Engvold et al, 2019; Basri, 2021).

The structure and dynamics of magnetic fields threading the atmospheres of stars other than the Sun are observed mostly indirectly. Magnetic field measurements from Zeeman splitting of photospheric spectral lines are becoming more accessible owing to instrumentation at optical and near-infrared wavelengths, such as CRIRES⁺ (Dorn et al, 2014), PEPSI (Strassmeier et al, 2015), ESPaDOnS (Donati et al, 2006), NARVAL (Aurière, 2003), HARPSpol (Snik et al, 2008; Piskunov et al, 2011), SPIRou (Donati et al, 2020), and CARMENES (Quirrenbach et al, 2014) and HPF (Mahadevan et al, 2012). This promotes reliable quantification of the magnetic flux and its heating mechanisms observable in indirect activity indicators, and their scaling laws

for different types of stars. We cover recent work on direct magnetic field measurements and their use in constraining the rotation-activity scalings in Section 2.

While our understanding is often driven by observations, numerical simulation frameworks are essential tools to better evaluate observational trends of stellar magnetic activity on cool stars. Forward modeling of observational diagnostics are mostly based on physical models developed originally for the Sun. Scaling laws are often used to extend the solar paradigm to younger and more active suns as well as for cooler stars with deeper convection zones. More physically motivated applications involve dynamo models of the global magnetic field and the flux emergence process as a function of stellar properties. We present some important recent developments in modeling photospheric diagnostics of stellar magnetism in Section 3.

The indirect diagnostics—also called proxies—of magnetic activity include: (1) disk-integrated brightness in intermediate and broad bandpasses for the effects on the photosphere; (2) narrow-band radiative fluxes centered on spectral lines such as H α and singly ionized Ca and Mg that probe the chromosphere; and (3) outer-atmospheric indicators of non-thermal heating by magnetic fields, at X-ray and radio wavelengths. We review recent advances in chromospheric and coronal proxies in relation to the long-term evolution of stellar activity in Section 4.

Stars with convective outer layers have dynamos that support large-scale fields from their interiors to their magnetospheric environments, also called astrospheres. Following star formation and disk dispersal, rapid stellar rotation coupled with convection leads to strong magnetic activity, which is responsible for strong magnetized winds removing angular momentum from the star. Rotational evolution of cool stars can be used as a proxy for the integrated large-scale field behavior. We discuss the connection between magnetic braking and global field properties in Section 5.

We propose strategies for further progress in the problems introduced above in Section 6.

2 Scaling of magnetic flux and non-thermal emission

Our picture of stellar magnetism and its influence on stellar evolution and activity is anchored in the detailed observational data from the Sun. Among other examples, the spatial correspondence between active regions and magnetic flux concentrations, the occurrence of faculae and dark spots along latitudinal bands, differential rotation, the thermal and magnetic structure of active regions, and the temporal variability including magnetic cycle(s), are phenomena that can be observed in the Sun (see, e.g., [Schrijver, 1987](#); [Solanki, 2003](#); [Solanki et al, 2006](#)). In analogy, they are assumed to occur on other stars (e.g., [Berdyugina, 2005](#)).

As a *direct* measurement of magnetic fields, we understand determination of the immediate influence of the field, e.g., the signatures of the Zeeman effect on line profiles. This is in contrast to *indirect* measurements, which include the measurement of proxies of magnetic activity, for example non-thermal emission. The direct measurement of magnetic fields is hampered by the fact that other stars are very far away and cannot be spatially resolved. One of the consequences is that spectroscopy can be obtained from the spatially integrated stars but not from individual areas, which leads to blending of spectroscopic effects caused by magnetism with those from other atmospheric effects and partial cancellation of polarization (see, e.g., [Donati and Landstreet, 2009](#); [Reiners, 2012](#); [Kochukhov, 2021](#)). Direct observations of magnetic fields therefore typically require substantial spectral resolution and signal-to-noise (S/N), and sometimes recurrent observations of the same star over different rotational phases. Therefore, other *indirect* indicators of stellar magnetism are often employed to characterize stellar magnetic activity. These are usually indicators of non-thermal emission that is generated by the stellar magnetic field in analogy to the solar example (see, e.g., [Reiners et al, 2022](#), and references therein).

Direct measurements of magnetism are usually those that investigate an immediate observable of the magnetic fields, i.e., spectroscopic signatures like the Zeeman effect. In solar-type and low-mass stars, the Zeeman effect causes the most often used *direct* signatures that are Zeeman broadening (observed in integrated light, Stokes *I*; [Saar, 1988](#)) and polarization (see, e.g., [Landi Degl'Innocenti and Landolfi, 2004](#)). Observational biases can be rather strong leading to large uncertainties in the measured field strengths and/or the amount of magnetism unseen by the observations (see, e.g., [Kochukhov and Reiners, 2020](#), and references therein) of several directions of polarization, and monitoring projects delivering very high S/N data have provided a wealth of information from direct field measurements.

Solar-type and low-mass stars show a clear relation between rotation and non-thermal emission observed in several activity indicators, e.g., X-rays ([Skumanich, 1972](#); [Noyes et al, 1984](#); [Pizzolato et al, 2003](#); [Wright et al, 2011](#); [Reiners et al, 2014](#)). The causal connection between stellar rotation, stellar activity, and rotational evolution is supposed to be (1) a mechanism providing more surface magnetic flux at high rotation rates in any given star, and (2) the generation of non-thermal emission in proportion to magnetic energy (or magnetic flux) at the stellar surface. Currently, there is no physical model that explains any of the two phenomena from first principles.

The relation between average surface magnetic flux density (or field strength, $\langle B \rangle$) and rotation is shown in [Fig. 1](#). Similar to the rotation-activity relation, the Rossby number, $Ro = P/\tau$ with τ the convective turnover time, is used as a normalized proxy of rotation. [Fig. 1](#) shows two regimes of magnetic fields: a group of rapid rotators with $Ro \leq 0.1$ and $\langle B \rangle > 1$ kG, and the slower rotators with significantly weaker fields. Both groups show a statistically significant relation between $\langle B \rangle$ and Ro . The dependence of $\langle B \rangle$ on Ro is

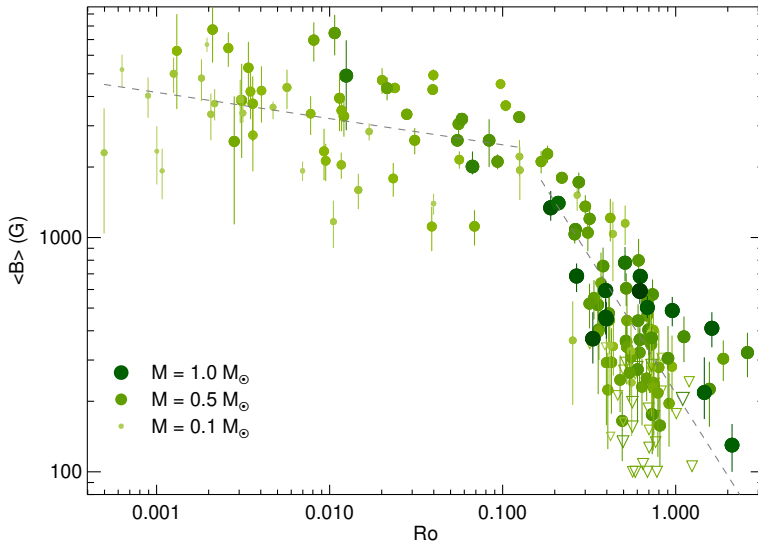


Fig. 1 Average surface magnetic field measurements from Stokes I in sun-like and low-mass stars (adapted from [Reiners et al, 2022](#)). Grey dashed lines indicate the relation between field strength and Rossby number, $Ro = P/\tau$, for two groups of “slow” and “fast” rotators. Stellar mass is indicated with symbol size and color, downward triangles indicate upper limits in $\langle B \rangle$.

a lot stronger among the slow rotators than within the more rapidly rotating group. The dashed lines show the relations:

$$\langle B \rangle = 199 \text{ G} \times Ro^{-1.26 \pm 0.10} \text{ for slow rotation} \quad (1)$$

$$\langle B \rangle = 2050 \text{ G} \times Ro^{-0.11 \pm 0.03} \text{ for rapid rotation} \quad (2)$$

The magnetic field-rotation relation (Fig. 1) closely resembles the rotation-activity relation mentioned above. This suggests that there is also a tight relation between magnetism and non-thermal emission. A relation between X-ray luminosity and magnetic flux was reported by [Pevtsov et al \(2003\)](#) and re-investigated for a sample of stars with measured surface fields by [Feiden and Chaboyer \(2013\)](#). Figure 2 shows relations between X-ray, $H\alpha$, and Ca H&K luminosity as a function of surface magnetic flux, Φ_B . All three luminosities significantly grow with Φ_B . It should be noted that both luminosity and magnetic flux scale with radius squared, implying that at least parts of the relations seen in Fig. 2 (and in [Pevtsov et al, 2003](#)) could be caused by the different radii. An analysis of magnetic flux density and normalized luminosities reveals that higher magnetic field strengths in fact cause stronger emission (see [Reiners et al, 2022](#)).

Figures 1 and 2 are adapted from [Reiners et al \(2022\)](#) and mainly cover M dwarf stars plus several young Suns from the literature. A broad range

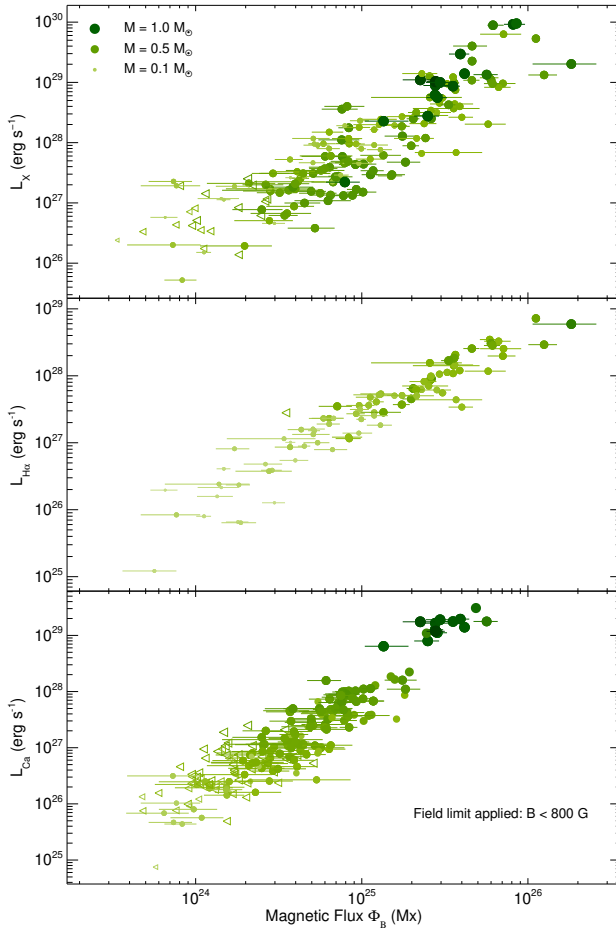


Fig. 2 Relations between magnetic flux, Φ_B , and total non-thermal emission as observed in X-rays (top panel), H α (center panel), and Ca H&K (bottom panel). Stellar mass is indicated with symbol size and color, leftward triangles indicate upper limits in $\langle B \rangle$. A maximum field strength of 800 G was used for the calculation of Φ_B in the bottom panel (see text and discussion in [Reiners et al, 2022](#)).

of stellar masses and rotation rates are included. The more rapidly rotating stars are observed to show stronger surface fields, and stellar surface magnetic flux leads to a proportional amount of non-thermal chromospheric and coronal emission. The Ca H&K lines show emission already at relatively low magnetic flux levels, and the field strength adopted for the calculation of Φ_B was limited to $\langle B \rangle < 800$ G indicating saturation of Ca H&K emission in very active stars (see [Reiners et al, 2022](#), for more details). Coronal X-ray emission requires a somewhat higher magnetic flux level to generate observable emission rates, and H α becomes visible in emission at similar or higher magnetic flux levels. The observed relations between magnetism and rotation, and between magnetism

and non-thermal emission provide a link between the wealth of information on stellar rotation and stellar activity. This should help to further constrain the processes of magnetic field generation and flux emergence in sun-like and low-mass stars.

An important property of stellar magnetic fields is its distribution across the stellar surface. Measurements of Zeeman broadening are sensitive to the integrated field across the stellar surface, but they are less sensitive to the distribution of individual field components. Measurements of polarized light in addition with observations taken at different times, with the goal of sampling the star at different rotational phases, can provide important information about the geometry of the field. The field measured in polarized light, in particular in the case of circular polarization only (Stokes V), resembles the distribution of the so-called large-scale field. This is because magnetic fields of opposite polarity can cancel each other and remain invisible to this type of observation. In general, results about the scaling of large-scale fields with stellar mass and rotation are consistent with observations of average surface fields and non-thermal emission (Vidotto et al, 2014).

Observations of large-scale fields have provided insight into magnetic geometries in very different stars (Donati and Landstreet, 2009; Marsden et al, 2014; Kochukhov, 2021). Additional information can be derived from the ratio between the large-scale field from circular polarization and the average field from Zeeman broadening. The ratio between Stokes V and Stokes I field strengths is typically on the order of 10% with individual stars showing up to 40% or less than 1% of their magnetic fields on large-scales. There is a slight trend of larger ratios $\langle B \rangle_V / \langle B \rangle_I$ occurring among the lower mass / smaller stars, which may indicate different modes of magnetic field generation but could also be influenced by biases in the observational methods. In addition to gathering more data on magnetic fields from Stokes V and I observations, it is very important to understand the systematic bias introduced by both methods. These include effects like unknown velocity fields and line profile distortions caused by non-thermal emission in Stokes I measurements, and the consequences of incomplete phase coverage, uncertainties of the inclination angle, and flux cancellation in Stokes V measurements.

3 Modeling photospheric magnetism

Magnetic features on stars other than the Sun can only be observed indirectly (except in a few cases with interferometry), as mentioned in Section 2. In essence, filling factors and distributions of starspots can only be inferred from disc-integrated diagnostics, often through data-driven modeling. Forward modeling (i.e., via numerical simulations) of surface magnetic features come into stage here, as they often bring physical insight that helps us interpret observations. This section is devoted to recent attempts in numerical simulations of observational diagnostics, based on physical models of magnetic flux generation and transport.

3.1 Distribution of surface magnetic flux

Attempts to model surface magnetic activity patterns on cool stars range from star-in-a-box simulations of convectively driven dynamos in M stars (e.g., [Yadav et al, 2015](#)) to solar-like models applied to stars rotating faster than the Sun, which we will focus on here.

The existence of polar or high-latitude spots on young solar-type stars rotating much faster than the Sun was revealed by Doppler imaging studies (e.g., [Strassmeier and Rice, 1998](#)). The formation and structure of near-polar spots is one of the problems in cool-star research. The main question is whether they emerge at near-polar latitudes, or are transported there by surface flows. There are two non-mutually exclusive explanations for such spot patterns in the literature. Firstly, any radially rising buoyant concentration of toroidal magnetic flux is expected to be deflected towards the rotation axis, owing to angular momentum conservation (or Coriolis force in the co-rotating frame), leading to poleward deflection that increases with the stellar rotation rate ([Schüssler and Solanki, 1992](#), see also [Weber et al. in this volume](#)). Numerical simulations of flux-tube emergence through the convection zone as a function of the stellar rotation rate provided further support for this hypothesis ([Schüssler et al, 1996](#)). According to the hypothesis, poleward deflection of rising tubes is controlled not only by the rotation rate, but also by the fractional depth of the convection zone (in turn, the Rossby number). A flux loop that starts from a low latitude and rises parallel to the rotation axis would thus have an emergence latitude that increases towards later spectral types as shown in simulations by [Granzer et al \(2000\)](#). The second explanation involves the transport of emerging flux by differential rotation, meridional flow and supergranulation ([Schrijver and Title, 2001](#)). Surface flux transport (SFT) simulations for various differential rotation and stellar radius configurations by [Işık et al \(2007\)](#) have shown that, mid-latitude emergence of highly tilted bipolar regions sustain polar spots, mainly by diffusion and meridional flow. Faster-than-solar meridional flow speeds were invoked by [Holzwarth et al \(2006\)](#), who showed formation of possible starspots with intermingled polarities around the rotational pole. All these studies showed various possibilities for the maintenance of long-lived polar spots by SFT processes.

Stellar dynamo models were incorporated to explain/simulate stellar cycle characteristics in addition to surface distributions. In a model that integrates a deep-seated dynamo, flux-tube rise and surface transport, [Işık et al \(2011\)](#) estimated the evolving surface distribution of large-scale radial magnetic flux through several dynamo cycles. They found that for intermediate rotators ($P_{\text{rot}} \sim 10$ d), the combined effects of enhanced cycle overlap and large tilt angles of emerging bipoles can lead to an unsigned-flux balance between polar caps and low latitudes that are modulated in anti-phase. This was suggested as an explanation for the existence of moderately active but non-cycling stars that were observed in S-index time series ([Hall and Lockwood, 2004](#)). For more extensive reviews of modeling work on stellar activity cycles, see [Biswas et al \(2023\)](#) and [Hazra et al \(2023\)](#).

Aiming to forward-model brightness variability in rotational time scales, [Işık et al \(2018\)](#) constructed a Flux Emergence and Transport (FEAT) simulation framework for solar-type stars with rotation rates and activity levels from the solar reference levels up to 8 times higher values. Assuming a solar-like latitudinal distribution of magnetic flux at the base of the convection zone, the authors modeled the surface emergence patterns by using simulations of buoyant flux tubes rising through the convection zone. The latitudes and tilt angles of emerging bipolar regions are used as input to a surface flux transport model, which calculates the time-dependent distribution of surface magnetic flux with a daily cadence, for a decade. The FEAT model also features active-region nesting at the time of emergence, with the probability that an active region emerges near the previous one being an adjustable parameter. They found that polar spots start to form between 4 and 8 times the solar rotation rate and activity level, by accumulation of trailing-polarity flux from tilted bipoles emerging at mid-latitudes. The tilt angles and thus the dipole contributions of emerging active regions increase in average, along with their variance around the mean ([Weber et al, 2023](#)). An enhanced nesting tendency locally increases the flux density reached in certain regions as well as in the formation of the spotted polar caps.

3.2 Line profile modeling

Despite the currently inaccessible detailed structure of stellar active regions, solar observations indicate that the magnetic field should be mostly radial upon emergence into the photosphere, owing to the steep density gradient in the atmosphere. Along with Gauss's law, this enforces a bipolar distribution of radial magnetic field throughout an active region. However, Zeeman-Doppler imaging (ZDI) studies indicate that, as the activity level increases, some rapidly rotating, young cool stars manifest strong azimuthal fields that can form axisymmetric bands (e.g., [Folsom et al, 2018](#)). The azimuthal field component tends to follow power laws with two different exponents on both sides of a stellar mass of about $0.5 M_{\odot}$, and it becomes more axisymmetric and confined to higher latitudes for more rapid rotators ([See et al, 2015](#)). Strong azimuthal fields on some stars much more active than the Sun was interpreted by [Solanki \(2002\)](#) as the effect of differential rotation acting on strong fields that accumulate or emerge near the rotational poles, resulting in amplification of azimuthal fields at mid-latitudes. Motivated by ZDI results, [Lehmann et al \(2017\)](#) decomposed simulated surface flux distributions into spherical harmonics, to obtain relative fractions of magnetic energy in radial, azimuthal, and meridional components (see [Vidotto, 2016](#), for a similar analysis for the Sun). They found that magnetic multipoles beyond the quadrupole (mainly contributed by azimuthal fields) host poloidal and toroidal field components following a fixed ratio. Later, [Lehmann et al \(2019\)](#) synthesised Stokes profiles from surface flux transport simulations for various activity levels and

concluded that ZDI overestimates the relative contributions from axisymmetric and toroidal fields, particularly as the axial inclination decreases towards pole-on configurations.

As a first application of the FEAT model described in Section 3.1, Şenavcı et al (2021) synthesised Doppler images of the young solar analogue EK Draconis, using SFT snapshots from the FEAT model, and compared them with the Doppler images they generated from observed spectra. The overall latitudinal distribution of spots in the simulations were consistent with the observations in the case of strong differential rotation, which was previously reported for EK Dra. The simulations also showed that low-latitude spots in observed Doppler images can result from mid-latitude activity in the partially visible rotational hemisphere, owing to the axial inclination of 63° . This study has shown the importance of forward modeling of the observed signals from physics-based models, in the interpretation of observations.

3.3 Brightness variability

Broad-band variability of cool stars on time scales ranging from the rotation period to the activity cycle result from photospheric manifestations of magnetic flux: mainly spots in active regions (ARs) and faculae resulting from AR network fields. Intriguingly, some solar-type stars with near-solar rotation rates and temperatures display unexpectedly large photometric variability amplitudes on the rotational time scale, in comparison to the Sun (Reinhold et al, 2020). By numerical simulations of light curves with different modes and degrees of active-region nesting, Işık et al (2020) showed that such high-amplitude light curves can be explained by a moderate increase of the emergence frequency and a high degree of nesting (up to 90%). The same study showed that active-longitude-type nesting can reproduce light-curve morphology of some stars with sinusoidal-like light curves in the same sample better than free nesting, where nests are allowed to form within active latitudes and a random longitude.

The Sun's brightness variability on the cycle timescale is dominated by bright faculae, because they cover larger areas despite their visibility being confined to near-limb regions in visible wavelengths. However, more active stars are known to get dimmer as they reach peak activity levels in their S-index time series (e.g., Radick et al, 1998). On the Sun, the area fractions of spots and faculae depend quadratically and linearly on the S-index, respectively. These dependencies can be used to predict that in more active stars, spots would dominate over faculae in terms of disc-area coverages and hence of brightness (Shapiro et al, 2014). The physical mechanism underlying this transition from facula-dominated to spot-dominated variability has been explained by Nèmec et al (2022), who carried out surface flux transport (SFT) simulations of a single solar-like activity cycle with gradually higher activity levels. The simulations were carried out for equator-on and pole-on inclinations. They showed qualitative agreement with the observed transition between facula- and spot-dominated cyclic variations of the solar-type sub-sample of Radick et al

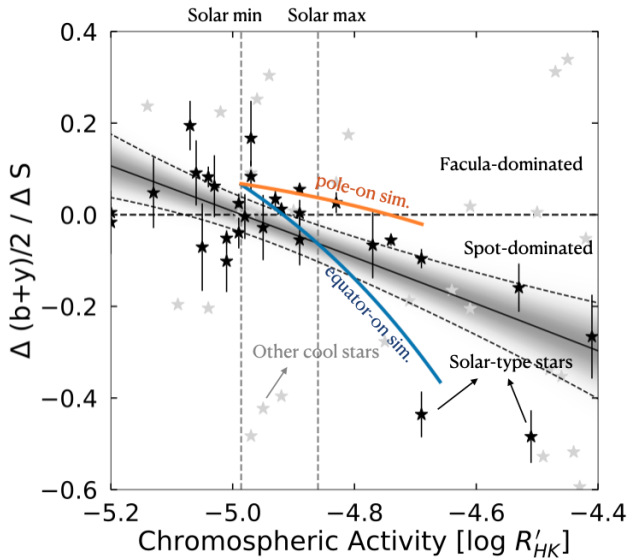


Fig. 3 Activity-related brightening (negative for dimming) as a function of the mean level of chromospheric activity in the HK bands. The stellar observations are shown by black stars (T_{eff} to within 200 K of the solar value and relative brightness uncertainty below 0.01) and gray stars corresponding to other stars in the sample of Radick et al (1998). The gray-shaded region shows the posterior distribution to 2σ of Bayesian linear regression to the near-solar sample, using Gaussian priors for a quadratic function. Blue and orange curves show the calculated brightening functions using SFT simulations, for equator-on and pole-on views, respectively.

(1998). Figure 3 shows the Strömgren $b + y$ brightening in units of the change (increase) in S-index as a function of $\log R'_{\text{HK}}$ for the stellar sample. Also shown are brightening estimates from a series of SFT simulations for two extreme axial inclinations. The expected transition from spot- to facula-dominated regime is not far from the current solar activity level during maxima. Here, the suggested mechanism for the transition is that for more active stars with presumably higher flux emergence rates, the active-region network field spanning much larger areas than sunspots finds more chance to undergo flux cancellation, owing to random superpositions of opposite magnetic polarities. On the Sun, the activity level is low enough to avoid such an overall flux cancellation effect, and the facular state remains the dominant counterpart, leading to a slight brightening of the Sun with increasing activity.

Physics-based forward modeling of light curves can help constrain the parameter space of stellar surface brightness distributions and the axial inclination. In such an attempt, the FEAT model (Section 3.1) was used to calculate synthetic light curves of G2V stars with rotation rates between Ω_{\odot} and $8\Omega_{\odot}$ (Němec et al, 2023). The method involved integration of facular and spot disc coverages weighted by the *Kepler* transmission function, evaluated at various axial inclinations. The results reproduced several observed characteristics of *Kepler* light curves of stars with different activity levels and variability

patterns. However, for a better match to observations and for an improved understanding of the observed change in stellar variability patterns as a function of the rotation rate, empirical relationships involving the magnetic flux emergence rate should be established and incorporated into models of flux emergence and transport.

3.4 Astrometric and radial velocity jitter

One promising method to infer activity-pattern characteristics is to make use of time-resolved high-precision astrometric measurements, exploiting the spatial symmetry breaking around the line of sight through the disc centre (Lanza et al, 2008). This lack of axial symmetry results from the fact that different portions of the disc have varying surface brightness. Based on a method developed by Shapiro et al (2021), numerical simulations of activity-induced astrometric jitter of solar-type stars were carried out by Sowmya et al (2021a) as a function of axial inclination, metallicity, and active-region nesting, finding that activity cycles can be inferred from systematic changes in the photocenter positions (see also Meunier et al, 2020). Moreover, when the degree of active-region nesting is high enough, the cyclic changes in the photocenter jitter can be detected by Gaia. Simulations for more active and rapidly rotating solar-type stars have shown that the jitter becomes spot-dominated and could be observed even on monthly timescales (Sowmya et al, 2022).

The radial velocity (RV) time series derived from photospheric absorption lines includes information on magnetic features as they transit the visible stellar disc, often hampering high-precision exoplanet detection with the same method. As part of a physics-based modeling framework of several activity indicators as a function of several stellar properties (Meunier et al, 2019), the radial velocity time series were also modelled by Meunier and Lagrange (2019). The RV variations led by magnetic features and their spatial distributions on the stellar disc showed general agreement with observations. The main features strongly affecting RV amplitudes were found to be the latitude coverage of active regions, the level of activity, and axial inclination.

4 Chromospheric and Coronal Activity

The most widely used indicator of chromospheric activity in solar-type stars is known as the S-index, which was devised in the late-1960s at Mount Wilson Observatory (Wilson, 1968). The S-index is a measurement of the stellar flux in the cores of the Ca II H and K spectral lines (N_H, N_K) relative to the flux in two neighboring pseudo-continuum bands (N_V, N_R).

$$S = \alpha \cdot \frac{N_H + N_K}{N_V + N_R}, \quad (3)$$

where α is a calibration constant that can be determined for any instrument using observations of standard stars monitored by the Mount Wilson survey

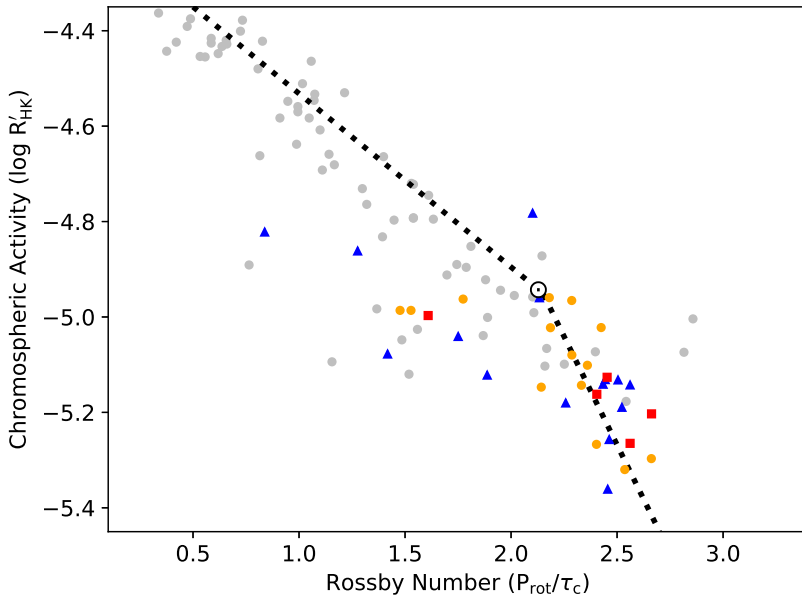


Fig. 4 The evolution of chromospheric activity with Rossby number for solar-type stars in the Mount Wilson survey (gray points) and for Kepler asteroseismic targets with precise Rossby numbers (colored points). Note the change in slope near the solar activity level.

(Vaughan et al, 1978). Time series measurements of the S-index for any given star can reveal variability due to stellar rotation and magnetic cycles (Jeffers et al, 2023). However, a meaningful comparison of stars with different spectral types requires a small correction for the photospheric contribution to the H and K emission, as well as a normalization by the bolometric luminosity (Noyes et al, 1984). This normalized activity indicator is known as R'_{HK} , and has been measured for thousands of solar-type stars (Boro Saikia et al, 2018).

The evolution of R'_{HK} over stellar lifetimes provides one method of estimating ages for isolated solar-type stars (Mamajek and Hillenbrand, 2008; Lorenzo-Oliveira et al, 2018). During the first half of their main-sequence lifetimes, the rotation rates and activity levels of solar-type stars appear to decline together roughly with the square-root of the age (Skumanich, 1972). At some critical value of the Rossby number ($\text{Ro} \equiv P_{\text{rot}}/\tau_c$) when the rotation period becomes comparable to the convective turnover time, rotation and activity become decoupled and the subsequent evolution of activity appears to be dominated by slow changes in the mechanical energy available from convection (Böhm-Vitense, 2007; Metcalfe et al, 2016). Figure 4 shows the rotation-activity relation for solar-type stars in the Mount Wilson survey (gray points; Baliunas et al, 1996) and for Kepler asteroseismic targets (colored points; Metcalfe et al, 2016). For the Mount Wilson stars, Rossby numbers have been calculated from $B - V$ colors (Noyes et al, 1984), and show a large scatter particularly at low activity levels ($\log R'_{\text{HK}} < -5$). For the Kepler targets, Rossby numbers have been calculated using turnover times near the base

of the convective envelope from an asteroseismic model for each star (Metcalf et al, 2014), including hotter F-type (blue triangles), sun-like G-type (yellow circles), and cooler K-type stars (red squares). Most of this sample appears to follow a common relation at low activity levels, possibly due to the higher precision of their Rossby numbers. Some outliers remain at lower Rossby number and higher activity level, perhaps from activity variations within an unknown magnetic cycle. Note that the rotation-activity relation is consistent with a change in slope near the solar activity level, which corresponds to the apparent onset of weakened magnetic braking (van Saders et al, 2016).

Modeling the chromospheric emission due to magnetic activity is important to better understand the physical characteristics of magnetism as a function of stellar properties. Such models would also be useful in disentangling various mechanisms that are likely responsible for generating the observed distributions of chromospheric emissions. Recently, Sowmya et al (2021b) developed a physics-based approach to forward-model S-index variations of the Sun as a star, from rotational to century-scale variations, but for the full range of the inclination of the rotation axis with respect to the line of sight. Based on their calculated S-index time series of the Sun for cycles 1-23, they found that the variability amplitude in the chromospheric emission of the Sun as seen from the full range of inclinations was representative of the variability distribution of other solar-type stars with similar $\langle R'_{\text{HK}} \rangle$, adapted from Radick et al (1998).

While magnetic heating of the chromosphere is evident in optical and ultraviolet spectral lines, similar processes heat the stellar corona to ~ 1 million K, emitting at X-ray wavelengths. A measurement of the X-ray luminosity is the coronal equivalent of the chromospheric S-index, and normalizing by the bolometric luminosity facilitates the comparison of stars with different spectral types like R'_{HK} . Depending on their evolutionary state, solar-type stars typically have a fractional X-ray luminosity $R_x \equiv L_x/L_{\text{bol}} \sim 10^{-3}$ to 10^{-8} (Schmitt and Liefke, 2004). Rather than decrease monotonically with rotation rate or Rossby number, there appear to be different regimes in the rotation-activity relation for X-rays. For the youngest and most rapidly rotating stars, there is a “saturated” regime in which R_x appears relatively constant for $\text{Ro} < 0.1$ (Pizzolato et al, 2003). It was initially unclear whether this saturation represented active regions filling the entire stellar surface, or a saturation of the underlying dynamo mechanism (Vilhu, 1984), but recent evidence suggests that it is a feature of the dynamo (Reiners et al, 2022). For stars with Rossby numbers between ~ 0.1 and the solar value, there is an “unsaturated” regime in which R_x decreases linearly with $\log \text{Ro}$, following a power law with an index $\beta \sim 2$ (Wright et al, 2011).

The evolution of X-ray luminosity for Rossby numbers greater than the solar value has been largely unexplored, with only a few measurements available at $R_x < 10^{-6}$. Considering the rotational and magnetic transitions that have recently been identified near the solar Rossby number (van Saders et al, 2016; Metcalfe et al, 2016), we can evaluate the currently available data from a new perspective. Rotation periods and X-ray luminosities are shown in Figure 5

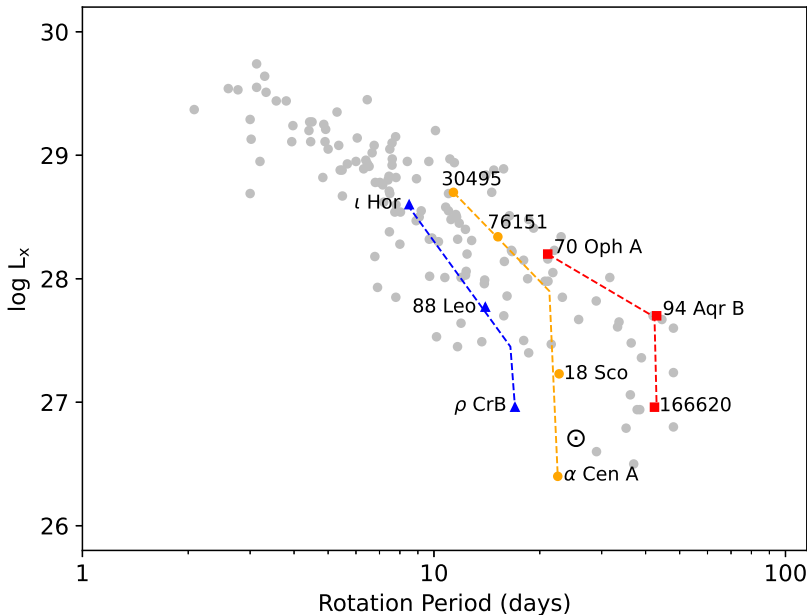


Fig. 5 The evolution of coronal activity with rotation for solar-type stars in the unsaturated regime (gray points; [Wright et al, 2011](#)), with evolutionary sequences of F-type (blue), G-type (yellow), and K-type stars (red) for comparison. The vertical tracks for older stars suggest a previously unrecognized “decoupled” regime in the rotation-activity relation.

for solar-type stars in the unsaturated regime (gray points; [Wright et al, 2011](#)), with evolutionary sequences of hotter F-type (blue triangles), sun-like G-type (yellow circles), and cooler K-type stars (red squares) for comparison. When stars reach the critical rotation period that corresponds to the onset of weakened magnetic braking for a given spectral type, the X-ray luminosity continues to decline at roughly constant rotation period. For example, despite having very similar rotation periods, the X-ray luminosities of the solar analogs 18 Sco (3.7 Gyr; [Li et al, 2012](#)) and α Cen A (5.4 Gyr; [Bazot et al, 2016](#)) differ by nearly an order of magnitude. This behavior suggests a previously unrecognized “decoupled” regime in the rotation-activity relation, where the X-ray luminosity is no longer determined by rotation.

5 Magnetic Braking

Magnetic braking is the loss of angular momentum (AM) through the interaction of stellar mass loss and magnetic fields. Stars with convective outer envelopes ($T_{\text{eff}} < 6250\text{K}$) and magnetic dynamos spin down over time due to angular momentum loss from magnetized winds ([Kraft, 1967](#); [Skumanich, 1972](#)). It represents a unique window into the magnetism of the Sun and stars because operates in a feedback loop: slower rotation leads to weaker magnetic fields, which lead to less AM loss via magnetized winds. It is therefore both

a consequence and a driver of magnetic evolution. Rotational evolution can occur over billion-year timescales, and represents one of the best tests of the integrated behavior of the large-scale magnetic fields of stars over stellar lifetimes. Spin-down is most directly a probe of the strength of the large-scale dipole (Weber and Davis, 1967; Kawaler, 1988), with only minor contributions from higher-order fields under specific conditions (See et al, 2019). However, observed rotational evolution depends on many interacting ingredients—the magnetic field, details of the mass loss and wind flow, initial rotation rates, and internal angular momentum redistribution—making the interpretation of rotational evolution in the context of magnetism a subtle task.

5.1 Modeling Magnetic Braking

A model of rotational evolution has three ingredients: 1) the braking law, which most directly probes the magnetic field behavior, 2) some assumption of the initial AM, and 3) a prescription for internal AM redistribution. Together, they predict rotational evolution as a function of time.

5.1.1 Braking laws

The main sequence (MS) is where magnetic braking has the largest impact on rotational evolution for single stars. Over the MS lifetime, the braking appears to be a strong function of the rotation velocity— $\frac{dJ}{dt} \sim \omega^3$ (Skumanich, 1972), which asymptotically forces convergence to a narrow range of rotation periods at a given time for a given stellar mass. This has the benefit of making the rotation rates of old stars insensitive to the significant (and for purposes here, uninteresting) spread in birth rotation periods. Observationally, this convergence happens first in the more massive stars and later in the low-mass stars, with open clusters showing tight, converged rotation sequences by a few hundred Myr around solar temperatures.

The standard $\frac{dJ}{dt} \propto \omega^3$ spin down results in a period-age relation that goes roughly as $P_{rot} \propto \sqrt{t}$ —so-called “Skumanich” spin down (Skumanich, 1972). Much of the literature on braking seeks to empirically constrain this period-age relation while being largely agnostic to the underlying physical mechanisms (Barnes, 2007, 2010; Mamajek and Hillenbrand, 2008; Angus et al, 2015). To use braking as a constraint on magnetic field behavior, we turn to physically motivated magnetic braking laws that follow the basic formalism of (Weber and Davis, 1967; Mestel, 1968) for angular momentum loss from magnetized stellar winds. The torque on a star is most simply written as:

$$\tau = \dot{M}\Omega\langle r_A \rangle^2, \quad (4)$$

where r_A is the Alfvén radius where magnetic Alfvén velocity and wind velocity are equivalent. The average radius defines the effective “lever arm” of the torque, and depends both on the strength and morphology of the magnetic field (Réville et al, 2015; Garraffo et al, 2016; Finley and Matt, 2018). In practice, the challenge in defining a braking law is in prescribing \dot{M} and B (as it

enters in r_A). Many authors choose to fix a magnetic field morphology and make some assumption about how the magnetic field scales with stellar properties, often in the form of a Rossby scaling (e.g. Kawaler, 1988; Krishnamurthi et al, 1997; van Saders and Pinsonneault, 2013; Matt et al, 2015). Modern braking laws increasingly draw their forms from $> 1D$ MHD simulations of mass loss entrained in a magnetized wind (e.g. Matt and Pudritz, 2008), but still fundamentally require some additional input of how B scales with stellar properties, and necessarily make strong assumptions about the nature of wind launching. For mass loss, authors commonly adopt either empirical (e.g. Wood et al, 2005, 2021) or theoretical scalings (Cranmer and Saar, 2011), but the choice remains a significant uncertainty.

5.1.2 Additional Ingredients

Stars are born with roughly two orders of magnitude of spread in their initial rotation periods (Irwin and Bouvier, 2009; Herbst et al, 2002), due both to stochasticity in the birth angular momentum itself and star-disk interactions that occur in the first few Myr of the star’s life (Matt and Pudritz, 2005; Shu et al, 1994; Koenigl, 1991). While rotational evolution in solar mass stars becomes insensitive to choices of initial conditions within a few hundred Myrs, lower mass stars may retain sensitivity for Gyrs (Gallet and Bouvier, 2015), complicating the interpretation of their rotation periods (Epstein and Pinsonneault, 2014; Roquette et al, 2021). Authors generally either consider a range of initial rotation periods motivated by those observed in the youngest open clusters, or “launch” their braking simulations from initial conditions defined by a benchmark cluster (see Somers et al, 2017; Epstein and Pinsonneault, 2014). There is some evidence that stellar environments may alter the distribution of initial periods (Coker et al, 2016; Roquette et al, 2021).

Many braking prescriptions make the simplest (and often reasonably correct) assumption that internal AM transport is instantaneous compared to evolutionary timescales, resulting in solid body rotation. However, the efficiency of internal AM transport does affect the evolution of the surface rotation period. Literature braking laws that allow for interior AM transport generally use either 1) simple “two-zone” models (MacGregor and Brenner, 1991) allow rotation of the core and convective envelope to evolve separately, coupled by AM transport over some characteristic timescale τ_{ce} , or 2) allow for extra AM transport via a diffusion term (Denissenkov et al, 2010; Somers and Pinsonneault, 2016; Spada and Lanzafame, 2020) in interiors models. There is no accepted first-principles mechanism for interior AM transport that fully reproduces observations. Magnetically mediated transport at the tachocline has been proposed (Oglethorpe and Garaud, 2013), as have internal gravity waves (Denissenkov et al, 2008; Fuller et al, 2014; Somers et al, 2017; Cao et al, 2023), but no conclusive mechanism has been identified.

5.2 Recent Modifications to Braking Laws

Because of the uncertainties in both the braking process and the fundamental underlying stellar processes of mass loss and magnetic field generation, all modern braking laws are tuned via fitting parameters to observations. Improvements in the underlying physical models come largely from examining whether the braking prescription captures the observed mass and time dependence of the spin down.

Observational benchmark systems must have both well-known ages and rotation periods. The most impactful class of calibrating systems to date has been the open clusters, which represent coeval stellar populations that span a range of masses at uniform composition. However, cluster calibrators have historically been confined to young ($< 1\text{Gyr}$) ages and solar composition stars; old open clusters are rare and tend to be distant and challenging to study. Although the lack of calibrating sources at low masses, old ages, and non-solar compositions remains a persistent roadblock in the testing and validation of magnetic braking models, two classes of new calibrator sources have fueled recent refinements of magnetic braking laws: intermediate-age open clusters observed with space- and ground-based photometric missions, and bright field stars with precise, asteroseismically measured ages. Both classes have suggested significant alterations to the Skumanich-type spin-down that we will discuss below.

We show a sample of calibrator stars selected to lie in a relatively narrow slice between $1.0 < M_{\odot} < 1.1$ and $0.0 < [\text{Fe}/\text{H}] < 0.2$ in Figure 6. These calibrators are shown against a braking law that includes 1) a range of initial conditions (gaussian centered at 8 days, with a 1σ width of 4 days), 2) disk-locking timescales drawn uniformly from 1-5 Myr, 3) the braking law form from [van Saders et al \(2016\)](#) with the addition of core-envelope decoupling following the [Somers and Pinsonneault \(2016\)](#) 2-zone model. Rough regions where different processes discussed in this section are important for interpreting the rotation period are noted, but readers should be aware that the exact boundaries of these regions are both mass and metallicity dependent.

5.2.1 Young Stars

Young open clusters retain a subset of rapidly rotating stars for hundreds of millions of years, longer than Skumanich-type spin-down law would predict given the simultaneous existence of slow rotators. This observation motivates the inclusion of an epoch of “saturated” spin down in nearly all magnetic braking models, in which the spin down instead goes as $\frac{dJ}{dt} \propto \omega_{crit}^2 \omega$ ([Krishnamurthi et al, 1997](#)). This saturated regime is the analog of saturation in other magnetic proxies: the observation that beyond some ω_{crit} more rapid rotation no longer results in a stronger magnetic response, in this case reflected in the angular momentum loss. In practice, the saturation threshold is often

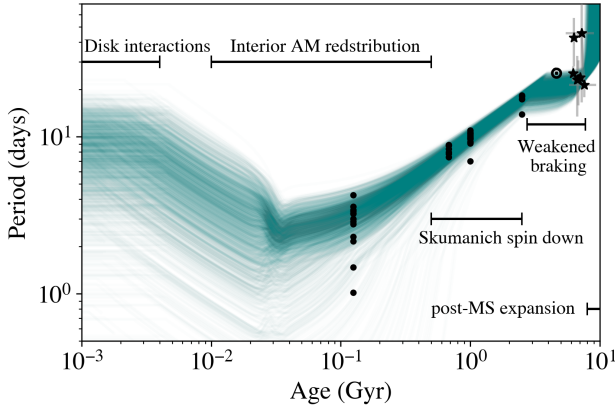


Fig. 6 Calibrator stars (points) of known rotation period and age shown against calibrated braking laws that include a range of initial conditions (teal tracks), internal AM redistribution, and weakened magnetic braking. Cluster stars (circles) are drawn from the compilation in Curtis et al (2020), and asteroseismic targets (stars) from van Saders et al (2016) and Hall et al (2021).

included as a Rossby scaling, with $Ro_{sat} \propto (\omega_{crit}\tau_{cz})^{-1}$. A saturation threshold of $Ro_{sat} \sim 0.1$ is broadly consistent both with the saturation threshold in other magnetic proxies, and with the observed rotational behavior in clusters.

5.2.2 Intermediate-Age Stars

In detailed cluster observations, spin-down rates depart from those expected for unsaturated, Skumanich-type spin-down in young and intermediate-age stars. Stars initially spin-down faster-than-expected (Denissenkov et al, 2010), and then “stalled out” at intermediate ages with what appears to be minimal evolution in the surface rotation rate (Agüeros et al, 2018; Curtis et al, 2020). Although we cannot entirely rule out changes to the magnetic braking itself as the cause, internal AM transport is emerging as a leading explanation. While the epoch of “core-envelope” decoupling is brief and subtle for solar mass stars (Denissenkov et al, 2010; Gallet and Bouvier, 2015), the apparently long timescales for transport in low-mass stars produces a stark pileup in the cluster sequences of 1 Gyr old open clusters (Curtis et al, 2020). There are also puzzling gaps in the distribution of cool field stars at periods just longward of feature, which may suggest a similar phenomenon in the population at large (Lu et al, 2022). Cao et al (2023) identified a magnetic counterpart to the observed rotational stalling, and showed that stars putatively undergoing core-envelope recoupling in the Praesepe open cluster had starkly elevated surface spot-filling fractions, which the authors argued is the consequence of the radial shears present during this epoch of AM redistribution. At a minimum, the spin-down evolution of intermediate-age stars is more complex than Skumanich; the exact mechanism (and magnetic involvement) remain areas of active inquiry.

5.2.3 Old Stars

Recent observations of bright field stars with precisely measured asteroseismic ages provide insight into rotation at a wider range of ages and compositions in solar mass stars. The seismic sample also displays non-Skumanich behavior: it traces the standard magnetic braking patterns at young and intermediate ages, but appears to undergo dramatically reduced angular momentum loss in the latter half of the main sequence lifetime (van Saders et al, 2016). Followup work showed that the observed long-period edge in the field star rotation distribution (McQuillan et al, 2014; Matt et al, 2015) was also consistent with weakened braking (van Saders et al, 2019; David et al, 2022), and that the weakened braking was apparent even when rotation rates were measured methods other than spot modulation (Hall et al, 2021; Masuda et al, 2022). These braking models allow for standard evolution until some critical Rossby number is reached— Ro_{crit} —after which the braking is severely reduced or AM loss truncated entirely. The mechanism again remains uncertain: van Saders et al (2016) and Metcalfe et al (2016) suggested that an overall weakening of the magnetic field strength and shift to higher-order morphologies could be responsible, and detailed studies of stars on either side of the transition have thus far supported the picture of weakening dipole fields as a driver for the change in spin-down (see Metcalfe et al, 2023, and references therein). However, changes in the mass loss rates, and details of the wind launching and flow are not ruled out.

6 Outlook

Because the underlying mechanisms are still poorly understood, progress in understanding stellar magnetism is very much driven by observations, and then theoretical efforts to reproduce the patterns we see. Larger, more complete, and more comprehensive datasets drive this progress. Those data are challenging to obtain—whether they be subtle spot signatures, direct measurements of weak fields, precise ages and rotation rates, or decades-long activity cycles—with significant progress in the last decade. There are two classes of observational benchmarks that enable progress: small, but exquisitely studied samples of stars with multiple precision measurements of magnetic proxies that allow us to build a complete picture of their behavior, and truly large but comparatively more poorly constrained samples that allow us to probe the properties and patterns in populations.

The various attempts at forward modeling of photospheric activity diagnostics are helpful in deepening our understanding of the physics of magnetic activity, along with qualitative comparisons with the available observations. Extending magnetic flux emergence and subsequent surface evolution models of spots and faculae to wide ranges of stellar properties (e.g., T_{eff} , differential rotation, metallicity) will be important in evaluating observational data. We note, however, that care should be taken when interpreting observations with the matching simulations. The inverse problem of recovering the surface

magnetic patterns is often ill-posed, involving several parameter degeneracies. Likelihood-free inference frameworks have the potential to illuminate parameter ranges that optimally simulate observed data, allowing a Bayesian way of inverting observations (e.g., Cranmer et al, 2020).

Models of magnetic braking have seen frequent, large revisions in recent years as new data become available. Because the number of calibrating sources still spans a relatively narrow range of masses, ages, and compositions, there is likely much to learn as new corners of parameter space become accessible. Observational improvements are likely to come from a combination of many datasets, with two paths for growth: 1) small samples with exceptional observational coverage (rotation, asteroseismology, magnetic activity cycle measurements, direct magnetic field mapping for all targets), and 2) very large but more poorly characterized stellar samples, enabled by large photometric, spectroscopic, and astrometric surveys. Pushing to lower masses, older ages, and less solar-like compositions are the most critical directions for new observational insight into braking behavior. On the theoretical side, progress can be made by increasingly ground braking models in first-principles or semi-empirical models of magnetized winds, and gradually phasing out the more purely empirical scalings currently in use (e.g., Chebly et al, 2023; Evensberger et al, 2023). As has been the case since the beginning of this field, the interplay between improved observational calibrator sets and more sophisticated physical models will drive progress.

Acknowledgments. This review was written following the workshop “Solar and Stellar Dynamos: A New Era”, hosted and supported by the International Space Science Institute (ISSI) in Bern, Switzerland. The authors wish to express their thanks to ISSI for their financial and logistical support.

Ethics Declarations

Competing interests The authors declare they have no conflicts of interest.

References

- Agüeros MA, Bowsher EC, Bochanski JJ, et al (2018) A New Look at an Old Cluster: The Membership, Rotation, and Magnetic Activity of Low-mass Stars in the 1.3 Gyr Old Open Cluster NGC 752. *Astrophys. J.* 862(1):33. <https://doi.org/10.3847/1538-4357/aac6ed>, <https://arxiv.org/abs/1804.02016> [astro-ph.SR]
- Angus R, Aigrain S, Foreman-Mackey D, et al (2015) Calibrating gyrochronology using Kepler asteroseismic targets. *Mon. Not. Roy. Astron. Soc.* 450(2):1787–1798. <https://doi.org/10.1093/mnras/stv423>, <https://arxiv.org/abs/1502.06965> [astro-ph.EP]

- Aurière M (2003) Stellar Polarimetry with NARVAL. In: Arnaud J, Meunier N (eds) EAS Publications Series, p 105
- Baliunas S, Sokoloff D, Soon W (1996) Magnetic Field and Rotation in Lower Main-Sequence Stars: an Empirical Time-dependent Magnetic Bode's Relation? *Astrophys. J. Lett.*457:L99. <https://doi.org/10.1086/309891>
- Barnes SA (2007) Ages for Illustrative Field Stars Using Gyrochronology: Viability, Limitations, and Errors. *Astrophys. J.*669(2):1167–1189. <https://doi.org/10.1086/519295>, <https://arxiv.org/abs/0704.3068> [astro-ph]
- Barnes SA (2010) A Simple Nonlinear Model for the Rotation of Main-sequence Cool Stars. I. Introduction, Implications for Gyrochronology, and Color-Period Diagrams. *Astrophys. J.*722(1):222–234. <https://doi.org/10.1088/0004-637X/722/1/222>
- Basri G (2021) *An Introduction to Stellar Magnetic Activity*. IOP Publishing, Bristol, <https://doi.org/10.1088/2514-3433/ac2956>
- Bazot M, Christensen-Dalsgaard J, Gizon L, et al (2016) On the uncertain nature of the core of α Cen A. *Mon. Not. Roy. Astron. Soc.*460(2):1254–1269. <https://doi.org/10.1093/mnras/stw921>, <https://arxiv.org/abs/1603.07583> [astro-ph.SR]
- Berdyugina SV (2005) Starspots: A Key to the Stellar Dynamo. *Living Reviews in Solar Physics* 2(1):8. <https://doi.org/10.12942/lrsp-2005-8>
- Biswas A, Karak BB, Usoskin I, et al (2023) Long-Term Modulation of Solar Cycles. *Space Sci. Rev.*219(3):19. <https://doi.org/10.1007/s11214-023-00968-w>, <https://arxiv.org/abs/2302.14845> [astro-ph.SR]
- Böhm-Vitense E (2007) Chromospheric Activity in G and K Main-Sequence Stars, and What It Tells Us about Stellar Dynamos. *Astrophys. J.*657(1):486–493. <https://doi.org/10.1086/510482>
- Boro Saikia S, Marvin CJ, Jeffers SV, et al (2018) Chromospheric activity catalogue of 4454 cool stars. Questioning the active branch of stellar activity cycles. *Astron. Astrophys.*616:A108. <https://doi.org/10.1051/0004-6361/201629518>, <https://arxiv.org/abs/1803.11123> [astro-ph.SR]
- Cao L, Pinsonneault MH, van Saders JL (2023) Core-envelope decoupling drives radial shear dynamos in cool stars. *arXiv e-prints* arXiv:2301.07716. <https://doi.org/10.48550/arXiv.2301.07716>, <https://arxiv.org/abs/2301.07716> [astro-ph.SR]
- Chebly JJ, Alvarado-Gómez JD, Poppenhäger K, et al (2023) Numerical quantification of the wind properties of cool main sequence stars. *Mon.*

- Not. Roy. Astron. Soc.524(4):5060–5079. <https://doi.org/10.1093/mnras/stad2100>, <https://arxiv.org/abs/2307.04615> [astro-ph.SR]
- Coker CT, Pinsonneault M, Terndrup DM (2016) Evidence for Cluster to Cluster Variations in Low-mass Stellar Rotational Evolution. *Astrophys. J.*833(1):122. <https://doi.org/10.3847/1538-4357/833/1/122>, <https://arxiv.org/abs/1604.05729> [astro-ph.SR]
- Cranmer K, Brehmer J, Louppe G (2020) The frontier of simulation-based inference. *Proceedings of the National Academy of Science* 117(48):30,055–30,062. <https://doi.org/10.1073/pnas.1912789117>, <https://arxiv.org/abs/1911.01429> [stat.ML]
- Cranmer SR, Saar SH (2011) Testing a Predictive Theoretical Model for the Mass Loss Rates of Cool Stars. *Astrophys. J.*741(1):54. <https://doi.org/10.1088/0004-637X/741/1/54>, <https://arxiv.org/abs/1108.4369> [astro-ph.SR]
- Curtis JL, Agüeros MA, Matt SP, et al (2020) When Do Stalled Stars Resume Spinning Down? Advancing Gyrochronology with Ruprecht 147. *Astrophys. J.*904(2):140. <https://doi.org/10.3847/1538-4357/abbf58>, <https://arxiv.org/abs/2010.02272> [astro-ph.SR]
- David TJ, Angus R, Curtis JL, et al (2022) Further Evidence of Modified Spindown in Sun-like Stars: Pileups in the Temperature-Period Distribution. *Astrophys. J.*933(1):114. <https://doi.org/10.3847/1538-4357/ac6dd3>, <https://arxiv.org/abs/2203.08920> [astro-ph.SR]
- Denissenkov PA, Pinsonneault M, MacGregor KB (2008) What Prevents Internal Gravity Waves from Disturbing the Solar Uniform Rotation? *Astrophys. J.*684(1):757–769. <https://doi.org/10.1086/589502>, <https://arxiv.org/abs/0801.3622> [astro-ph]
- Denissenkov PA, Pinsonneault M, Terndrup DM, et al (2010) Angular Momentum Transport in Solar-type Stars: Testing the Timescale for Core-Envelope Coupling. *Astrophys. J.*716(2):1269–1287. <https://doi.org/10.1088/0004-637X/716/2/1269>, <https://arxiv.org/abs/0911.1121> [astro-ph.SR]
- Donati JF, Landstreet JD (2009) Magnetic Fields of Nondegenerate Stars. *Annual Review of Astron. and Astrophys.*47:333–370. <https://doi.org/10.1146/annurev-astro-082708-101833>, <https://arxiv.org/abs/0904.1938> [astro-ph.SR]
- Donati JF, Catala C, Landstreet JD, et al (2006) ESPaDOnS: The New Generation Stellar Spectro-Polarimeter. Performances and First Results. In: Casini R, Lites BW (eds) *Solar Polarization 4*, p 362

- Donati JF, Kouach D, Moutou C, et al (2020) SPIRou: NIR velocimetry and spectropolarimetry at the CFHT. *Mon. Not. Roy. Astron. Soc.*498(4):5684–5703. <https://doi.org/10.1093/mnras/staa2569>, <https://arxiv.org/abs/2008.08949> [astro-ph.IM]
- Dorn RJ, Anglada-Escude G, Baade D, et al (2014) CRIRES+: Exploring the Cold Universe at High Spectral Resolution. *The Messenger* 156:7–11
- Engvold O, Vial JC, Skumanich A (2019) The Sun as a Guide to Stellar Physics. Elsevier, Amsterdam, <https://doi.org/10.1016/C2017-0-01365-4>
- Epstein CR, Pinsonneault MH (2014) How Good a Clock is Rotation? The Stellar Rotation-Mass-Age Relationship for Old Field Stars. *Astrophys. J.*780(2):159. <https://doi.org/10.1088/0004-637X/780/2/159>, <https://arxiv.org/abs/1203.1618> [astro-ph.SR]
- Evensberget D, Marsden SC, Carter BD, et al (2023) The winds of young Solar-type stars in the Pleiades, AB Doradus, Columba, and β Pictoris. *Mon. Not. Roy. Astron. Soc.*524(2):2042–2063. <https://doi.org/10.1093/mnras/stad1650>, <https://arxiv.org/abs/2305.17427> [astro-ph.SR]
- Feiden GA, Chaboyer B (2013) Magnetic Inhibition of Convection and the Fundamental Properties of Low-mass Stars. I. Stars with a Radiative Core. *Astrophys. J.*779(2):183. <https://doi.org/10.1088/0004-637X/779/2/183>, <https://arxiv.org/abs/1309.0033> [astro-ph.SR]
- Finley AJ, Matt SP (2018) The Effect of Combined Magnetic Geometries on Thermally Driven Winds. II. Dipolar, Quadrupolar, and Octupolar Topologies. *Astrophys. J.*854(2):78. <https://doi.org/10.3847/1538-4357/aaaab5>, <https://arxiv.org/abs/1801.07662> [astro-ph.SR]
- Folsom CP, Bouvier J, Petit P, et al (2018) The evolution of surface magnetic fields in young solar-type stars II: the early main sequence (250-650 Myr). *Mon. Not. Roy. Astron. Soc.*474(4):4956–4987. <https://doi.org/10.1093/mnras/stx3021>, <https://arxiv.org/abs/1711.08636> [astro-ph.SR]
- Fuller J, Lecoanet D, Cantiello M, et al (2014) Angular Momentum Transport via Internal Gravity Waves in Evolving Stars. *Astrophys. J.*796(1):17. <https://doi.org/10.1088/0004-637X/796/1/17>, <https://arxiv.org/abs/1409.6835> [astro-ph.SR]
- Gallet F, Bouvier J (2015) Improved angular momentum evolution model for solar-like stars. II. Exploring the mass dependence. *Astron. Astrophys.*577:A98. <https://doi.org/10.1051/0004-6361/201525660>, <https://arxiv.org/abs/1502.05801> [astro-ph.SR]

- Garraffo C, Drake JJ, Cohen O (2016) The missing magnetic morphology term in stellar rotation evolution. *Astron. Astrophys.*595:A110. <https://doi.org/10.1051/0004-6361/201628367>, <https://arxiv.org/abs/1607.06096> [astro-ph.SR]
- Granzer T, Schüssler M, Caligari P, et al (2000) Distribution of starspots on cool stars. II. Pre-main-sequence and ZAMS stars between 0.4 M_{sun} and 1.7 M_{sun} . *Astron. Astrophys.*355:1087–1097
- Hall JC, Lockwood GW (2004) The Chromospheric Activity and Variability of Cycling and Flat Activity Solar-Analog Stars. *Astrophys. J.*614(2):942–946. <https://doi.org/10.1086/423926>
- Hall OJ, Davies GR, van Saders J, et al (2021) Weakened magnetic braking supported by asteroseismic rotation rates of Kepler dwarfs. *Nature Astronomy* 5:707–714. <https://doi.org/10.1038/s41550-021-01335-x>, <https://arxiv.org/abs/2104.10919> [astro-ph.SR]
- Hazra G, Nandy D, Kitchatinov L, et al (2023) Mean Field Models of Flux Transport Dynamo and Meridional Circulation in the Sun and Stars. *Space Sci. Rev.*219(5):39. <https://doi.org/10.1007/s11214-023-00982-y>, <https://arxiv.org/abs/2302.09390> [astro-ph.SR]
- Herbst W, Bailer-Jones CAL, Mundt R, et al (2002) Stellar rotation and variability in the Orion Nebula Cluster. *Astron. Astrophys.*396:513–532. <https://doi.org/10.1051/0004-6361:20021362>
- Holzwarth V, Mackay DH, Jardine M (2006) The impact of meridional circulation on stellar butterfly diagrams and polar caps. *Mon. Not. Roy. Astron. Soc.*369(4):1703–1718. <https://doi.org/10.1111/j.1365-2966.2006.10407.x>, <https://arxiv.org/abs/astro-ph/0604102> [astro-ph]
- Işık E, Schüssler M, Solanki SK (2007) Magnetic flux transport on active cool stars and starspot lifetimes. *Astron. Astrophys.*464(3):1049–1057. <https://doi.org/10.1051/0004-6361:20066623>, <https://arxiv.org/abs/astro-ph/0612399> [astro-ph]
- Işık E, Schmitt D, Schüssler M (2011) Magnetic flux generation and transport in cool stars. *Astron. Astrophys.*528:A135. <https://doi.org/10.1051/0004-6361/201014501>, <https://arxiv.org/abs/1102.0569> [astro-ph.SR]
- Işık E, Solanki SK, Krivova NA, et al (2018) Forward modelling of brightness variations in Sun-like stars. I. Emergence and surface transport of magnetic flux. *Astron. Astrophys.*620:A177. <https://doi.org/10.1051/0004-6361/201833393>, <https://arxiv.org/abs/1810.06728> [astro-ph.SR]
- Işık E, Shapiro AI, Solanki SK, et al (2020) Amplification of Brightness

- Variability by Active-region Nesting in Solar-like Stars. *Astrophys. J. Lett.*901(1):L12. <https://doi.org/10.3847/2041-8213/abb409>, <https://arxiv.org/abs/2009.00692> [astro-ph.SR]
- Irwin J, Bouvier J (2009) The rotational evolution of low-mass stars. In: Mamajek EE, Soderblom DR, Wyse RFG (eds) *The Ages of Stars*, pp 363–374, <https://doi.org/10.1017/S1743921309032025>, 0901.3342
- Jeffers SV, Kiefer R, Metcalfe TS (2023) Stellar Activity Cycles. arXiv e-prints arXiv:2309.14138. <https://doi.org/10.48550/arXiv.2309.14138>, <https://arxiv.org/abs/2309.14138> [astro-ph.SR]
- Kawaler SD (1988) Angular Momentum Loss in Low-Mass Stars. *Astrophys. J.*333:236. <https://doi.org/10.1086/166740>
- Kochukhov O (2021) Magnetic fields of M dwarfs. *Astron. Astrophys. Reviews*29(1):1. <https://doi.org/10.1007/s00159-020-00130-3>, <https://arxiv.org/abs/2011.01781> [astro-ph.SR]
- Kochukhov O, Reiners A (2020) The Magnetic Field of the Active Planet-hosting M Dwarf AU Mic. *Astrophys. J.*902(1):43. <https://doi.org/10.3847/1538-4357/abb2a2>, <https://arxiv.org/abs/2008.10668> [astro-ph.SR]
- Koenigl A (1991) Disk Accretion onto Magnetic T Tauri Stars. *Astrophys. J. Lett.*370:L39. <https://doi.org/10.1086/185972>
- Kraft RP (1967) Studies of Stellar Rotation. V. The Dependence of Rotation on Age among Solar-Type Stars. *Astrophys. J.*150:551. <https://doi.org/10.1086/149359>
- Krishnamurthi A, Pinsonneault MH, Barnes S, et al (1997) Theoretical Models of the Angular Momentum Evolution of Solar-Type Stars. *Astrophys. J.*480(1):303–323. <https://doi.org/10.1086/303958>
- Landi Degl'Innocenti E, Landolfi M (2004) Polarization in Spectral Lines, vol 307. Springer, Dordrecht, <https://doi.org/10.1007/978-1-4020-2415-3>
- Lanza AF, De Martino C, Rodonò M (2008) Astrometric effects of solar-like magnetic activity in late-type stars and their relevance for the detection of extrasolar planets. *New Astronomy* 13(2):77–84. <https://doi.org/10.1016/j.newast.2007.06.009>, <https://arxiv.org/abs/0706.2942> [astro-ph]
- Lehmann LT, Jardine MM, Vidotto AA, et al (2017) The energy budget of stellar magnetic fields: comparing non-potential simulations and observations. *Mon. Not. Roy. Astron. Soc.*466(1):L24–L28. <https://doi.org/10.1093/mnrasl/slw225>, <https://arxiv.org/abs/1610.08314> [astro-ph.SR]

- Lehmann LT, Hussain GAJ, Jardine MM, et al (2019) Observing the simulations: applying ZDI to 3D non-potential magnetic field simulations. *Mon. Not. Roy. Astron. Soc.*483(4):5246–5266. <https://doi.org/10.1093/mnras/sty3362>, <https://arxiv.org/abs/1811.03703> [astro-ph.SR]
- Li TD, Bi SL, Liu K, et al (2012) Stellar parameters and seismological analysis of the star 18 Scorpii. *Astron. Astrophys.*546:A83. <https://doi.org/10.1051/0004-6361/201219063>
- Lorenzo-Oliveira D, Freitas FC, Meléndez J, et al (2018) The Solar Twin Planet Search. The age-chromospheric activity relation. *Astron. Astrophys.*619:A73. <https://doi.org/10.1051/0004-6361/201629294>, <https://arxiv.org/abs/1806.08014> [astro-ph.SR]
- Lu YL, Curtis JL, Angus R, et al (2022) Bridging the Gap-The Disappearance of the Intermediate Period Gap for Fully Convective Stars, Uncovered by New ZTF Rotation Periods. *Astron. J.*164(6):251. <https://doi.org/10.3847/1538-3881/ac9bee>, <https://arxiv.org/abs/2210.06604> [astro-ph.SR]
- MacGregor KB, Brenner M (1991) Rotational Evolution of Solar-Type Stars. I. Main-Sequence Evolution. *Astrophys. J.*376:204. <https://doi.org/10.1086/170269>
- Mahadevan S, Ramsey L, Bender C, et al (2012) The habitable-zone planet finder: a stabilized fiber-fed NIR spectrograph for the Hobby-Eberly Telescope. In: McLean IS, Ramsay SK, Takami H (eds) *Ground-based and Airborne Instrumentation for Astronomy IV*, p 84461S, <https://doi.org/10.1117/12.926102>, 1209.1686
- Mamajek EE, Hillenbrand LA (2008) Improved Age Estimation for Solar-Type Dwarfs Using Activity-Rotation Diagnostics. *Astrophys. J.*687(2):1264–1293. <https://doi.org/10.1086/591785>, <https://arxiv.org/abs/0807.1686> [astro-ph]
- Marsden SC, Petit P, Jeffers SV, et al (2014) A BCool magnetic snapshot survey of solar-type stars. *Mon. Not. Roy. Astron. Soc.*444(4):3517–3536. <https://doi.org/10.1093/mnras/stu1663>, <https://arxiv.org/abs/1311.3374> [astro-ph.SR]
- Masuda K, Petigura EA, Hall OJ (2022) Inferring the rotation period distribution of stars from their projected rotation velocities and radii: Application to late-F/early-G Kepler stars. *Mon. Not. Roy. Astron. Soc.*510(4):5623–5638. <https://doi.org/10.1093/mnras/stab3650>, <https://arxiv.org/abs/2112.07162> [astro-ph.SR]
- Matt S, Pudritz RE (2005) Accretion-powered Stellar Winds as a Solution to the Stellar Angular Momentum Problem. *Astrophys. J.*

- Lett.632(2):L135–L138. <https://doi.org/10.1086/498066>, <https://arxiv.org/abs/astro-ph/0510060> [astro-ph]
- Matt S, Pudritz RE (2008) Accretion-powered Stellar Winds. II. Numerical Solutions for Stellar Wind Torques. *Astrophys. J.*678(2):1109–1118. <https://doi.org/10.1086/533428>, <https://arxiv.org/abs/0801.0436> [astro-ph]
- Matt SP, Brun AS, Baraffe I, et al (2015) The Mass-dependence of Angular Momentum Evolution in Sun-like Stars. *Astrophys. J. Lett.*799(2):L23. <https://doi.org/10.1088/2041-8205/799/2/L23>, <https://arxiv.org/abs/1412.4786> [astro-ph.SR]
- McQuillan A, Mazeh T, Aigrain S (2014) Rotation Periods of 34,030 Kepler Main-sequence Stars: The Full Autocorrelation Sample. *Astrophys. J. Supplement*211(2):24. <https://doi.org/10.1088/0067-0049/211/2/24>, <https://arxiv.org/abs/1402.5694> [astro-ph.SR]
- Mestel L (1968) Magnetic braking by a stellar wind-I. *Mon. Not. Roy. Astron. Soc.*138:359. <https://doi.org/10.1093/mnras/138.3.359>
- Metcalfe TS, Creevey OL, Doğan G, et al (2014) Properties of 42 Solar-type Kepler Targets from the Asteroseismic Modeling Portal. *Astrophys. J. Supplement*214(2):27. <https://doi.org/10.1088/0067-0049/214/2/27>, <https://arxiv.org/abs/1402.3614> [astro-ph.SR]
- Metcalfe TS, Egeland R, van Saders J (2016) Stellar Evidence That the Solar Dynamo May Be in Transition. *Astrophys. J. Lett.*826(1):L2. <https://doi.org/10.3847/2041-8205/826/1/L2>, <https://arxiv.org/abs/1606.01926> [astro-ph.SR]
- Metcalfe TS, Strassmeier KG, Ilyin IV, et al (2023) Constraints on Magnetic Braking from the G8 Dwarf Stars 61 UMa and τ Cet. *Astrophys. J. Lett.*948(1):L6. <https://doi.org/10.3847/2041-8213/acce38>, <https://arxiv.org/abs/2304.09896> [astro-ph.SR]
- Meunier N, Lagrange AM (2019) Activity time series of old stars from late F to early K. II. Radial velocity jitter and exoplanet detectability. *Astron. Astrophys.*628:A125. <https://doi.org/10.1051/0004-6361/201935347>, <https://arxiv.org/abs/1909.02969> [astro-ph.SR]
- Meunier N, Lagrange AM, Boulet T, et al (2019) Activity time series of old stars from late F to early K. I. Simulating radial velocity, astrometry, photometry, and chromospheric emission. *Astron. Astrophys.*627:A56. <https://doi.org/10.1051/0004-6361/201834796>, <https://arxiv.org/abs/1904.01437> [astro-ph.SR]
- Meunier N, Lagrange AM, Borgniet S (2020) Activity time series of old stars

- from late F to early K. V. Effect on exoplanet detectability with high-precision astrometry. *Astron. Astrophys.*644:A77. <https://doi.org/10.1051/0004-6361/202038710>, <https://arxiv.org/abs/2011.02158> [astro-ph.SR]
- Nèmec NE, Shapiro AI, Işık E, et al (2022) Faculae Cancel out on the Surfaces of Active Suns. *Astrophys. J. Lett.*934(2):L23. <https://doi.org/10.3847/2041-8213/ac8155>, <https://arxiv.org/abs/2207.06816> [astro-ph.SR]
- Nèmec NE, Shapiro AI, Işık E, et al (2023) Forward modelling of brightness variations in Sun-like stars. II. Light curves and variability. *Astron. Astrophys.*672:A138. <https://doi.org/10.1051/0004-6361/202244412>, <https://arxiv.org/abs/2303.03040> [astro-ph.SR]
- Noyes RW, Hartmann LW, Baliunas SL, et al (1984) Rotation, convection, and magnetic activity in lower main-sequence stars. *Astrophys. J.*279:763–777. <https://doi.org/10.1086/161945>
- Oglethorpe RLF, Garaud P (2013) Spin-down Dynamics of Magnetized Solar-type Stars. *Astrophys. J.*778(2):166. <https://doi.org/10.1088/0004-637X/778/2/166>, <https://arxiv.org/abs/1401.0932> [astro-ph.SR]
- Pevtsov AA, Fisher GH, Acton LW, et al (2003) The Relationship Between X-Ray Radiance and Magnetic Flux. *Astrophys. J.*598:1387–1391. <https://doi.org/10.1086/378944>
- Piskunov N, Snik F, Dolgoplov A, et al (2011) HARPSpol — The New Polarimetric Mode for HARPS. *The Messenger* 143:7–10
- Pizzolato N, Maggio A, Micela G, et al (2003) The stellar activity-rotation relationship revisited: Dependence of saturated and non-saturated X-ray emission regimes on stellar mass for late-type dwarfs. *Astron. Astrophys.*397:147–157. <https://doi.org/10.1051/0004-6361:20021560>
- Quirrenbach A, Amado PJ, Caballero JA, et al (2014) CARMENES instrument overview. In: Ramsay SK, McLean IS, Takami H (eds) *Ground-based and Airborne Instrumentation for Astronomy V*, p 91471F, <https://doi.org/10.1117/12.2056453>
- Radick RR, Lockwood GW, Skiff BA, et al (1998) Patterns of Variation among Sun-like Stars. *Astrophys. J. Supplement*118(1):239–258. <https://doi.org/10.1086/313135>
- Reiners A (2012) Observations of Cool-Star Magnetic Fields. *Living Reviews in Solar Physics* 9:1. <https://arxiv.org/abs/1203.0241> [astro-ph.SR]
- Reiners A, Schüssler M, Passegger VM (2014) Generalized Investigation of the Rotation-Activity Relation: Favoring Rotation Period instead of Rossby

- Number. *Astrophys. J.*794(2):144. <https://doi.org/10.1088/0004-637X/794/2/144>, <https://arxiv.org/abs/1408.6175> [astro-ph.SR]
- Reiners A, Shulyak D, Käpylä PJ, et al (2022) Magnetism, rotation, and non-thermal emission in cool stars. Average magnetic field measurements in 292 M dwarfs. *Astron. Astrophys.*662:A41. <https://doi.org/10.1051/0004-6361/202243251>, <https://arxiv.org/abs/2204.00342> [astro-ph.SR]
- Reinhold T, Shapiro AI, Solanki SK, et al (2020) The Sun is less active than other solar-like stars. *Science* 368(6490):518–521. <https://doi.org/10.1126/science.aay3821>, <https://arxiv.org/abs/2005.01401> [astro-ph.SR]
- Réville V, Brun AS, Matt SP, et al (2015) The Effect of Magnetic Topology on Thermally Driven Wind: Toward a General Formulation of the Braking Law. *Astrophys. J.*798(2):116. <https://doi.org/10.1088/0004-637X/798/2/116>, <https://arxiv.org/abs/1410.8746> [astro-ph.SR]
- Roquette J, Matt SP, Winter AJ, et al (2021) The influence of the environment on the spin evolution of low-mass stars - I. External photoevaporation of circumstellar discs. *Mon. Not. Roy. Astron. Soc.*508(3):3710–3729. <https://doi.org/10.1093/mnras/stab2772>, <https://arxiv.org/abs/2109.10296> [astro-ph.SR]
- Saar SH (1988) Improved Methods for the Measurement and Analysis of Stellar Magnetic Fields. *Astrophys. J.*324:441. <https://doi.org/10.1086/165907>
- Schmitt JHMM, Liefke C (2004) NEXXUS: A comprehensive ROSAT survey of coronal X-ray emission among nearby solar-like stars. *Astron. Astrophys.*417:651–665. <https://doi.org/10.1051/0004-6361:20030495>, <https://arxiv.org/abs/astro-ph/0308510> [astro-ph]
- Schrijver CJ (1987) Solar active regions - Radiative intensities and large-scale parameters of the magnetic field. *Astron. Astrophys.*180(1-2):241–252
- Schrijver CJ, Title AM (2001) On the Formation of Polar Spots in Sun-like Stars. *Astrophys. J.*551(2):1099–1106. <https://doi.org/10.1086/320237>
- Schrijver CJ, Zwaan C (2000) *Solar and Stellar Magnetic Activity*. Cambridge University Press, Cambridge
- Schüssler M, Solanki SK (1992) Why rapid rotators have polar spots. *Astron. Astrophys.*264:L13–L16
- Schüssler M, Caligari P, Ferriz-Mas A, et al (1996) Distribution of starspots on cool stars. I. Young and main sequence stars of $1M_{sun}$ -. *Astron. Astrophys.*314:503–512

- See V, Jardine M, Vidotto AA, et al (2015) The energy budget of stellar magnetic fields. *Mon. Not. Roy. Astron. Soc.*453(4):4301–4310. <https://doi.org/10.1093/mnras/stv1925>, <https://arxiv.org/abs/1508.01403> [astro-ph.SR]
- See V, Matt SP, Finley AJ, et al (2019) Do Non-dipolar Magnetic Fields Contribute to Spin-down Torques? *Astrophys. J.*886(2):120. <https://doi.org/10.3847/1538-4357/ab46b2>, <https://arxiv.org/abs/1910.02129> [astro-ph.SR]
- Şenavcı HV, Kılıçoğlu T, Işık E, et al (2021) Observing and modelling the young solar analogue EK Draconis: starspot distribution, elemental abundances, and evolutionary status. *Mon. Not. Roy. Astron. Soc.*502(3):3343–3356. <https://doi.org/10.1093/mnras/stab199>, <https://arxiv.org/abs/2101.07248> [astro-ph.SR]
- Shapiro AI, Solanki SK, Krivova NA, et al (2014) Variability of Sun-like stars: reproducing observed photometric trends. *Astron. Astrophys.*569:A38. <https://doi.org/10.1051/0004-6361/201323086>, <https://arxiv.org/abs/1406.2383> [astro-ph.SR]
- Shapiro AI, Solanki SK, Krivova NA (2021) Predictions of Astrometric Jitter for Sun-like Stars. I. The Model and Its Application to the Sun as Seen from the Ecliptic. *Astrophys. J.*908(2):223. <https://doi.org/10.3847/1538-4357/abd630>, <https://arxiv.org/abs/2012.12312> [astro-ph.SR]
- Shu F, Najita J, Ostriker E, et al (1994) Magnetocentrifugally Driven Flows from Young Stars and Disks. I. A Generalized Model. *Astrophys. J.*429:781. <https://doi.org/10.1086/174363>
- Skumanich A (1972) Time Scales for Ca II Emission Decay, Rotational Braking, and Lithium Depletion. *Astrophys. J.*171:565. <https://doi.org/10.1086/151310>
- Snik F, Jeffers S, Keller C, et al (2008) The upgrade of HARPS to a full-Stokes high-resolution spectropolarimeter. In: McLean IS, Casali MM (eds) *Ground-based and Airborne Instrumentation for Astronomy II*, p 701400, <https://doi.org/10.1117/12.787393>
- Solanki SK (2002) The magnetic structure of sunspots and starspots. *Astronomische Nachrichten* 323:165–177. [https://doi.org/10.1002/1521-3994\(200208\)323:3/4<165::AID-ASNA165>3.0.CO;2-U](https://doi.org/10.1002/1521-3994(200208)323:3/4<165::AID-ASNA165>3.0.CO;2-U)
- Solanki SK (2003) Sunspots: An overview. *Astron. Astrophys. Reviews*11(2-3):153–286. <https://doi.org/10.1007/s00159-003-0018-4>
- Solanki SK, Inhester B, Schüssler M (2006) The solar magnetic field. *Reports on Progress in Physics* 69(3):563–668. <https://doi.org/10.1088/0034-4885/69/3/R02>, <https://arxiv.org/abs/1008.0771> [astro-ph.SR]

- Somers G, Pinsonneault MH (2016) Lithium Depletion is a Strong Test of Core-envelope Recoupling. *Astrophys. J.*829(1):32. <https://doi.org/10.3847/0004-637X/829/1/32>, <https://arxiv.org/abs/1606.00004> [astro-ph.SR]
- Somers G, Stauffer J, Rebull L, et al (2017) M Dwarf Rotation from the K2 Young Clusters to the Field. I. A Mass-Rotation Correlation at 10 Myr. *Astrophys. J.*850(2):134. <https://doi.org/10.3847/1538-4357/aa93ed>, <https://arxiv.org/abs/1710.07638> [astro-ph.SR]
- Sowmya K, Nèmec NE, Shapiro AI, et al (2021a) Predictions of Astrometric Jitter for Sun-like Stars. II. Dependence on Inclination, Metallicity, and Active-region Nesting. *Astrophys. J.*919(2):94. <https://doi.org/10.3847/1538-4357/ac111b>, <https://arxiv.org/abs/2107.01493> [astro-ph.SR]
- Sowmya K, Shapiro AI, Witzke V, et al (2021b) Modeling Stellar Ca II H and K Emission Variations. I. Effect of Inclination on the S-index. *Astrophys. J.*914(1):21. <https://doi.org/10.3847/1538-4357/abf247>, <https://arxiv.org/abs/2103.13893> [astro-ph.SR]
- Sowmya K, Nèmec NE, Shapiro AI, et al (2022) Predictions of Astrometric Jitter for Sun-like Stars. III. Fast Rotators. *Astrophys. J.*934(2):146. <https://doi.org/10.3847/1538-4357/ac79b3>, <https://arxiv.org/abs/2206.07702> [astro-ph.SR]
- Spada F, Lanzafame AC (2020) Competing effect of wind braking and interior coupling in the rotational evolution of solar-like stars. *Astron. Astrophys.*636:A76. <https://doi.org/10.1051/0004-6361/201936384>, <https://arxiv.org/abs/1908.00345> [astro-ph.SR]
- Strassmeier KG (2009) Starspots. *Astron. Astrophys. Reviews*17(3):251–308. <https://doi.org/10.1007/s00159-009-0020-6>
- Strassmeier KG, Rice JB (1998) Doppler imaging of stellar surface structure. VI. HD 129333 = EK Draconis: a stellar analog of the active young Sun. *Astron. Astrophys.*330:685–695
- Strassmeier KG, Ilyin I, Järvinen A, et al (2015) PEPsi: The high-resolution échelle spectrograph and polarimeter for the Large Binocular Telescope. *Astronomische Nachrichten* 336(4):324. <https://doi.org/10.1002/asna.201512172>, <https://arxiv.org/abs/1505.06492> [astro-ph.IM]
- van Saders JL, Pinsonneault MH (2013) Fast Star, Slow Star; Old Star, Young Star: Subgiant Rotation as a Population and Stellar Physics Diagnostic. *Astrophys. J.*776(2):67. <https://doi.org/10.1088/0004-637X/776/2/67>, <https://arxiv.org/abs/1306.3701> [astro-ph.SR]
- van Saders JL, Ceillier T, Metcalfe TS, et al (2016) Weakened magnetic

- braking as the origin of anomalously rapid rotation in old field stars. *Nature* 529(7585):181–184. <https://doi.org/10.1038/nature16168>, <https://arxiv.org/abs/1601.02631> [astro-ph.SR]
- van Saders JL, Pinsonneault MH, Barbieri M (2019) Forward Modeling of the Kepler Stellar Rotation Period Distribution: Interpreting Periods from Mixed and Biased Stellar Populations. *Astrophys. J.* 872(2):128. <https://doi.org/10.3847/1538-4357/aafafe>, <https://arxiv.org/abs/1803.04971> [astro-ph.SR]
- Vaughan AH, Preston GW, Wilson OC (1978) Flux measurements of Ca II and K emission. *Pub. Astron. Soc. Pacific* 90:267–274. <https://doi.org/10.1086/130324>
- Vidotto AA (2016) The magnetic field vector of the Sun-as-a-star. *Mon. Not. Roy. Astron. Soc.* 459(2):1533–1542. <https://doi.org/10.1093/mnras/stw758>, <https://arxiv.org/abs/1603.09226> [astro-ph.SR]
- Vidotto AA, Gregory SG, Jardine M, et al (2014) Stellar magnetism: empirical trends with age and rotation. *Mon. Not. Roy. Astron. Soc.* 441(3):2361–2374. <https://doi.org/10.1093/mnras/stu728>, <https://arxiv.org/abs/1404.2733> [astro-ph.SR]
- Vilhu O (1984) The nature of magnetic activity in lower main sequence stars. *Astron. Astrophys.* 133:117–126
- Weber EJ, Davis J Leverett (1967) The Angular Momentum of the Solar Wind. *Astrophys. J.* 148:217–227. <https://doi.org/10.1086/149138>
- Weber MA, Schunker H, Jouve L, et al (2023) Understanding Active Region Emergence and Origins on the Sun and Other Cool Stars. arXiv e-prints arXiv:2306.06536. <https://doi.org/10.48550/arXiv.2306.06536>, <https://arxiv.org/abs/2306.06536> [astro-ph.SR]
- Wilson OC (1968) Flux Measurements at the Centers of Stellar H- and K-Lines. *Astrophys. J.* 153:221. <https://doi.org/10.1086/149652>
- Wood BE, Müller HR, Zank GP, et al (2005) New Mass-Loss Measurements from Astrospheric Ly α Absorption. *Astrophys. J. Lett.* 628(2):L143–L146. <https://doi.org/10.1086/432716>, <https://arxiv.org/abs/astro-ph/0506401> [astro-ph]
- Wood BE, Müller HR, Redfield S, et al (2021) New Observational Constraints on the Winds of M dwarf Stars. *Astrophys. J.* 915(1):37. <https://doi.org/10.3847/1538-4357/abfda5>, <https://arxiv.org/abs/2105.00019> [astro-ph.SR]
- Wright NJ, Drake JJ, Mamajek EE, et al (2011) The Stellar-activity-Rotation

Relationship and the Evolution of Stellar Dynamos. *Astrophys. J.*743(1):48. <https://doi.org/10.1088/0004-637X/743/1/48>, <https://arxiv.org/abs/1109.4634> [astro-ph.SR]

Yadav RK, Christensen UR, Morin J, et al (2015) Explaining the Coexistence of Large-scale and Small-scale Magnetic Fields in Fully Convective Stars. *Astrophys. J. Lett.*813(2):L31. <https://doi.org/10.1088/2041-8205/813/2/L31>, <https://arxiv.org/abs/1510.05541> [astro-ph.SR]